

**Electronic Supporting Information for
Theoretical Study of Vibronic Interactions in the Photoelectron
Spectra of Al₆N⁻**

Rishabh Kumar Pandey¹, Korutla Srikanth¹, Anuj Tak¹,
Abhishek Kumar² and Tammineni Rajagopala Rao¹

*Department of Chemistry, Indian Institute of
Technology Patna, Bihta, Bihar, India 801106 and
Indian Association for Cultivation of Science,
Kolkata, West Bengal, India 700032**

* rajgopal@iitp.ac.in

Table S.I. Bond lengths for Al_6N (in Å unit) obtained using CAM-B3LYP, M06-2X and MP2 level of theories with a 6-311+g(d) basis set.

Parameter	CAM-B3LYP	M06-2X	MP2
N ₁ -Al ₂	2.3529	2.3402	2.3514
N ₁ -Al ₄	1.9848	1.9869	1.9973
N ₁ -Al ₃	2.3543	2.3416	2.3527
N ₁ -Al ₇	1.9845	1.9865	1.9968
Al ₂ -Al ₃	2.5918	2.5717	2.6057
Al ₄ -Al ₅	2.9704	2.9644	2.9635
Al ₄ -Al ₇	2.5920	2.6055	2.6297
Al ₃ -Al ₆	2.6508	2.6414	2.66243

Table S.II. Quadratic and higher-order coupling parameters for \tilde{X}^2B_1 state. The parameters are given in the eV unit.

Vibrational mode frequencies	E_0	γ	C
$\nu_6 (a_2)$	0.0077	2.4260	-0.0042
$\nu_7 (a_2)$	0.0229	2.4248	-0.0066
$\nu_8 (a_2)$	0.0303	2.4250	-0.0040
$\nu_9 (b_1)$	0.0233	2.4265	0.0047
$\nu_{10} (b_1)$	0.0337	2.4246	-0.0064
$\nu_{11} (b_1)$	0.0661	2.4261	-0.0041
$\nu_{12} (b_2)$	0.0098	2.4252	-0.0095
$\nu_{13} (b_2)$	0.0132	2.4251	-0.0042
$\nu_{14} (b_2)$	0.0310	2.4251	-0.0049
$\nu_{15} (b_2)$	0.0650	2.4251	-0.0001
			-0.000002

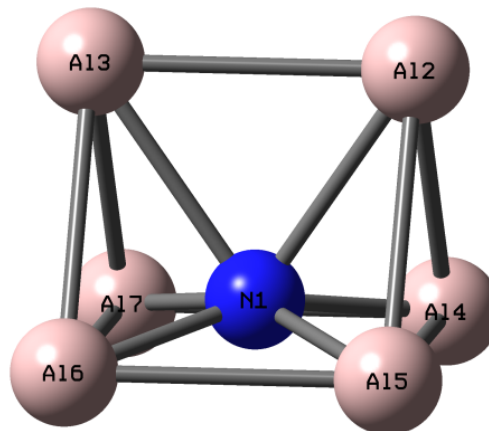


Figure S1. The optimized structure of neutral Al_6N .

Table S.III. Quadratic and higher-order coupling parameters for \tilde{A}^2A_1 state. The parameters are given in the eV unit.

Vibrational mode frequencies	E_0	γ	C
$\nu_6 (a_2)$	0.0077	3.1676	-0.0118
$\nu_7 (a_2)$	0.0229	3.1682	-0.0044
$\nu_8 (a_2)$	0.0303	3.1678	-0.0050
$\nu_9 (b_1)$	0.0233	3.1671	-0.0088
$\nu_{10} (b_1)$	0.0337	3.1673	-0.0046
$\nu_{11} (b_1)$	0.0661	3.1649	-0.0157
$\nu_{12} (b_2)$	0.0098	3.1589	-0.0673 0.0016
$\nu_{13} (b_2)$	0.0132	3.1647	-0.0454 0.0008
$\nu_{14} (b_2)$	0.0310	3.1671	-0.0223 0.0003
$\nu_{15} (b_2)$	0.0650	3.1643	-0.0569 0.0009

Table S.IV. Quadratic and higher-order coupling parameter for \tilde{B}^2B_2 state. The parameters are given in the eV unit.

Vibrational mode frequencies	E_0	γ
$\nu_6 (a_2)$	0.0077	3.2787 0.0140
$\nu_7 (a_2)$	0.0229	3.2784 0.0019
$\nu_8 (a_2)$	0.0303	3.2782 -0.0047
$\nu_9 (b_1)$	0.0233	3.2780 -0.0078
$\nu_{10} (b_1)$	0.0337	3.2780 -0.0016
$\nu_{11} (b_1)$	0.0661	3.2776 -0.0091
$\nu_{12} (b_2)$	0.0098	3.2934 0.0642
$\nu_{13} (b_2)$	0.0132	3.2840 0.0251
$\nu_{14} (b_2)$	0.0310	3.2800 0.0122
$\nu_{15} (b_2)$	0.0650	3.2808 0.0193

Table S.V. Quadratic and higher-order coupling parameters for \tilde{C}^2A_2 state. The parameters are given in the eV unit.

Vibrational mode frequencies	E_0	γ	δ	C
$\nu_6 (a_2)$	0.0077	4.2158	0.0033	
$\nu_7 (a_2)$	0.0229	4.2123	-0.0093	
$\nu_8 (a_2)$	0.0303	4.2151	-0.0043	
$\nu_9 (b_1)$	0.0233	4.2147	-0.0139	0.0001
$\nu_{10} (b_1)$	0.0337	4.2153	-0.0082	0.00002
$\nu_{11} (b_1)$	0.0661	4.2142	-0.0110	0.0001
$\nu_{12} (b_2)$	0.0098	4.2154	-0.0019	
$\nu_{13} (b_2)$	0.0132	4.2148	-0.0072	
$\nu_{14} (b_2)$	0.0310	4.2152	-0.0068	0.00003
$\nu_{15} (b_2)$	0.0650	4.2019	-0.0942	0.0014

Table S.VI. Quadratic and higher-order coupling parameters for \tilde{D}^2B_1 state. The parameters are given in the eV unit.

Vibrational mode frequencies	E_0	γ
$\nu_6 (a_2)$	0.0077	4.2007 -0.0010
$\nu_7 (a_2)$	0.0229	4.2005 -0.0009
$\nu_8 (a_2)$	0.0303	4.1989 -0.0010
$\nu_9 (b_1)$	0.0233	4.2008 0.0202
$\nu_{10} (b_1)$	0.0337	4.2012 0.0077
$\nu_{11} (b_1)$	0.0661	4.2035 0.0105
$\nu_{12} (b_2)$	0.0098	4.2014 0.0013
$\nu_{13} (b_2)$	0.0132	4.2009 0.0021
$\nu_{14} (b_2)$	0.0310	4.2033 0.0168
$\nu_{15} (b_2)$	0.0650	4.5246 0.0051

Table S.VII. Quadratic and higher-order coupling parameters for $\tilde{E}^2 A_1$ state. The parameters are given in the eV unit.

Vibrational mode frequencies	E_0	γ
$\nu_6 (a_2)$	0.0077	4.5310 0.0005
$\nu_7 (a_2)$	0.0229	4.5326 0.0049
$\nu_8 (a_2)$	0.0303	4.5310 0.0051
$\nu_9 (b_1)$	0.0233	4.5305 0.0005
$\nu_{10} (b_1)$	0.0337	4.5273 0.0153
$\nu_{11} (b_1)$	0.0661	4.5294 0.0242
$\nu_{12} (b_2)$	0.0098	4.5277 -0.0162
$\nu_{13} (b_2)$	0.0132	4.511 -0.0124
$\nu_{14} (b_2)$	0.0310	4.5297 0.0007
$\nu_{15} (b_2)$	0.0650	4.2696 0.0536

Table S.VIII. Quadratic and higher-order coupling parameters for $\tilde{F}^2 B_2$ state. The parameters are given in the eV unit.

Vibrational mode frequencies	E_0	γ
$\nu_6 (a_2)$	0.0077	4.7526 -0.0004
$\nu_7 (a_2)$	0.0229	4.7527 0.0096
$\nu_8 (a_2)$	0.0303	4.7532 0.0142
$\nu_9 (b_1)$	0.0233	4.7591 0.0276
$\nu_{10} (b_1)$	0.0337	4.7534 0.0092
$\nu_{11} (b_1)$	0.0661	4.7610 0.0298
$\nu_{12} (b_2)$	0.0098	4.7541 0.0021
$\nu_{13} (b_2)$	0.0132	4.7693 0.0289
$\nu_{14} (b_2)$	0.0310	4.7541 0.0126
$\nu_{15} (b_2)$	0.0650	4.7630 0.0237

Table S.IX. Normal modes combination, size of the primitive basis and single particle function (SPF) for uncoupled and coupled (TD and TI) calculations of Al_6N^- using the MCTDH approach.

Combination of normal modes	Primitive basis	SPF
ν_2	8	[12,12,12,12,12,12]
ν_1, ν_3	8,10	[10,10,10,10,10,10]
ν_4	10	[9,9,9,9,9,9]
ν_5	8	[7,7,7,7,7,7]
$\nu_2, \nu_6, \nu_{12}, \nu_{13}$	10,10,10,10	[12,12,12,12,12,12]
$\nu_1, \nu_3, \nu_7, \nu_8, \nu_9$	8,8,8,8,8,	[10,10,10,10,10,10]
$\nu_5, \nu_{10}, \nu_{11}, \nu_{14}, \nu_{15}, \nu_4$	6,6,6,6,6,6	[8,8,8,8,8,8]
ν_2	12	[12,12,12,12,12,12]
ν_1, ν_3	8,10	[10,10,10,10,10,10]
ν_4	10	[9,9,9,9,9,9]
ν_5	8	[7,7,7,7,7,7]
ν_2, ν_6, ν_{12}	8,8,8	[6,6,6,6,6,6]
$\nu_1, \nu_3, \nu_7, \nu_9$	6,6,6,6	[5,5,5,5,5,5]
ν_5, ν_4	5,5	[3,3,3,3,3,3]

Table S.X. Vibronic level assignments for fundamental and first overtone excitation (in cm^{-1}) of tuning modes for \tilde{A} state.

No.	Vibronic Energy Level	Assignments
1	0	0
2	280	ν_1
3	352	ν_2
4	542	ν_3
5	547	ν_4
6	633	ν_5
7	716	$2\nu_2$

Table S.XI. Vibronic level assignments for fundamental excitation (in cm^{-1}) of tuning modes for \tilde{B} state.

No.	Vibronic Energy Level	Assignments
1	0	0
2	261	ν_1
3	683	ν_2
4	808	ν_3
5	915	ν_4
6	924	ν_5

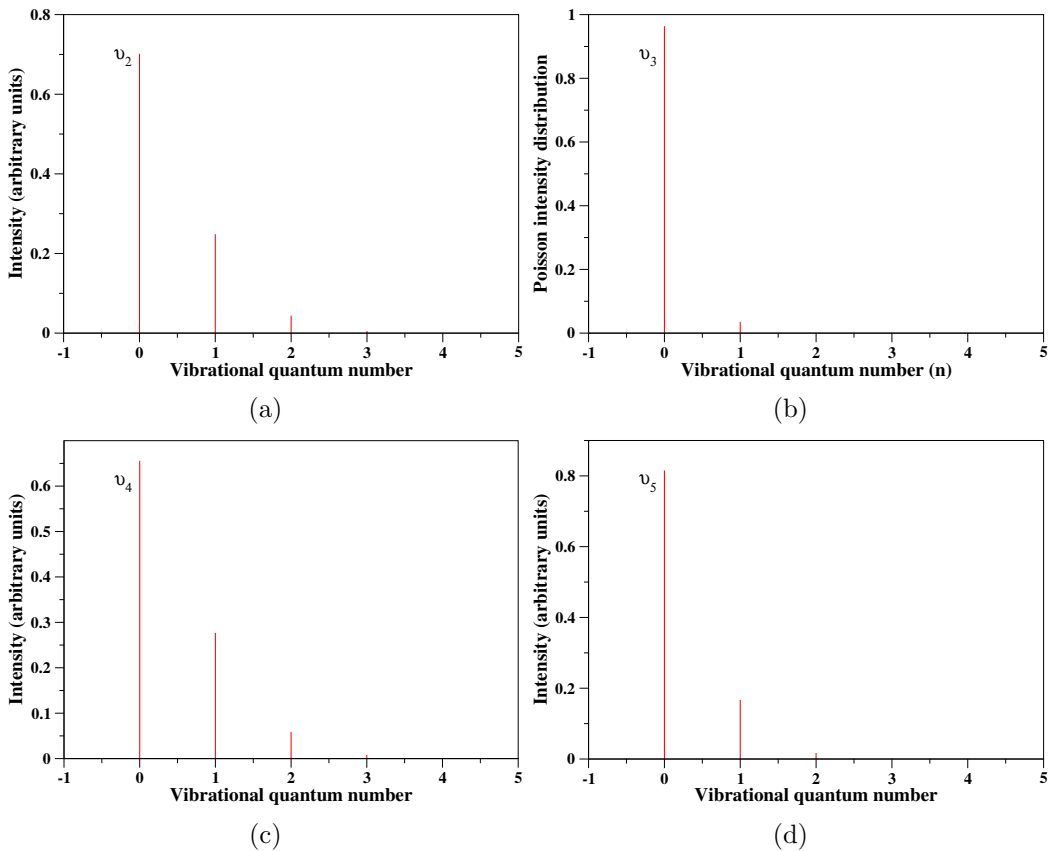


Figure S2. Poisson intensity distribution for tuning vibrational modes of \tilde{X}^2B_1 electronic state of Al₆N along vibrational quantum number.

Table S.XII. Vibronic level assignments for fundamental excitation (in cm^{-1}) of tuning modes for \tilde{C} state.

No.	Vibronic Energy Level	Assignments
1	0	0
2	551	ν_2
3	693	ν_4

Table S.XIII. Vibronic level assignments for fundamental excitation (in cm^{-1}) of tuning modes for \tilde{D} state.

No.	Vibronic Energy Level	Assignments
1	0	0
2	473	ν_2
3	547	ν_3

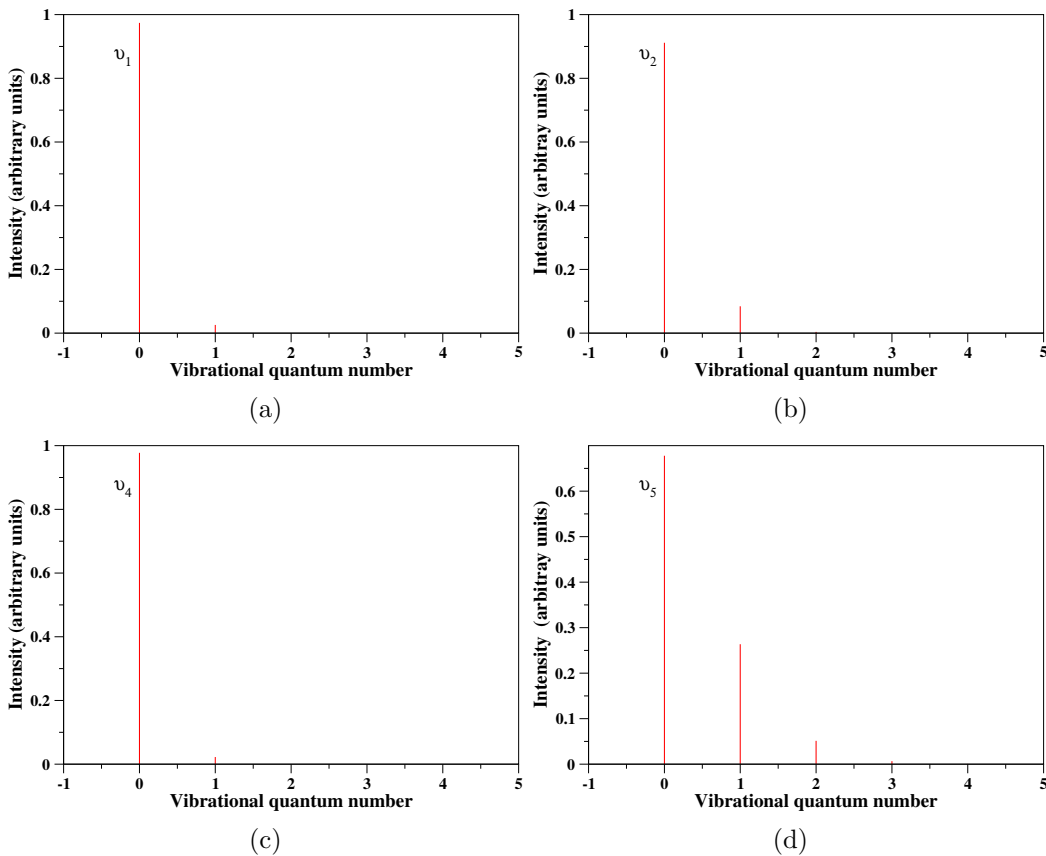


Figure S3. Poisson intensity distribution for tuning vibrational modes of \tilde{A}^2A_1 electronic state of Al₆N along vibrational quantum number.

Table S.XIV. Vibronic level assignments for fundamental excitation (in cm^{-1}) of tuning modes for \tilde{E} state.

No.	Vibronic Energy Level	Assignments
1	0	0
2	545	ν_2
3	984	ν_5

Table S.XV. Vibronic level assignments for fundamental excitation (in cm^{-1}) of tuning modes for \tilde{F} state.

No.	Vibronic Energy Level	Assignments
1	0	0
2	208	ν_1
3	358	ν_3
4	488	ν_4
5	538	ν_5

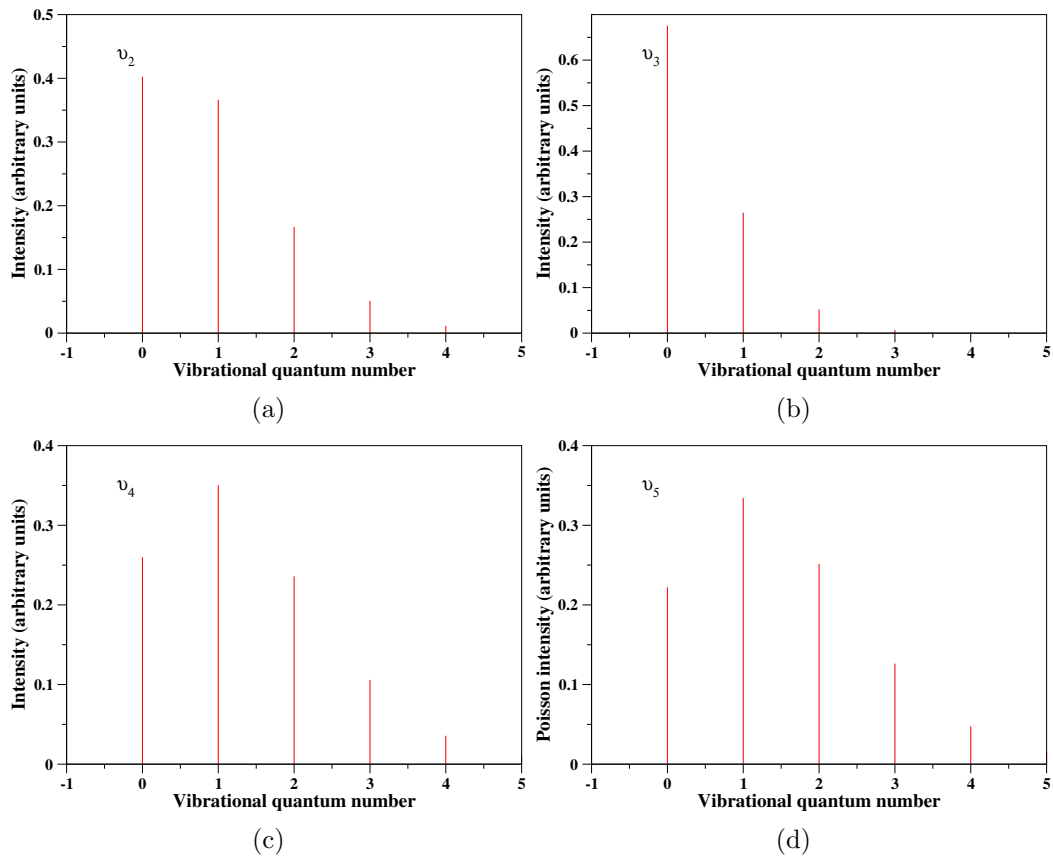


Figure S4. Poisson intensity distribution for tuning vibrational modes of \tilde{B}^2B_2 electronic state of Al_6N along vibrational quantum number.

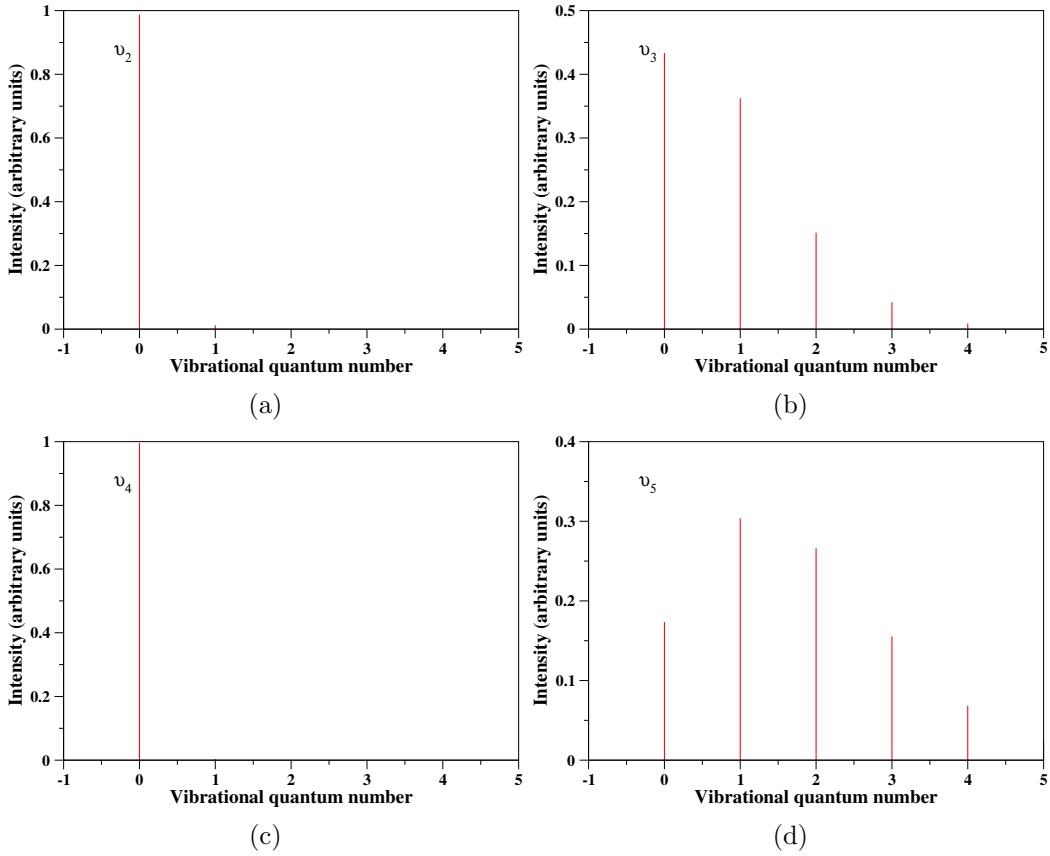


Figure S5. Poisson intensity distribution for tuning modes of \tilde{C}^2A_2 electronic state of Al_6N along vibrational quantum number.

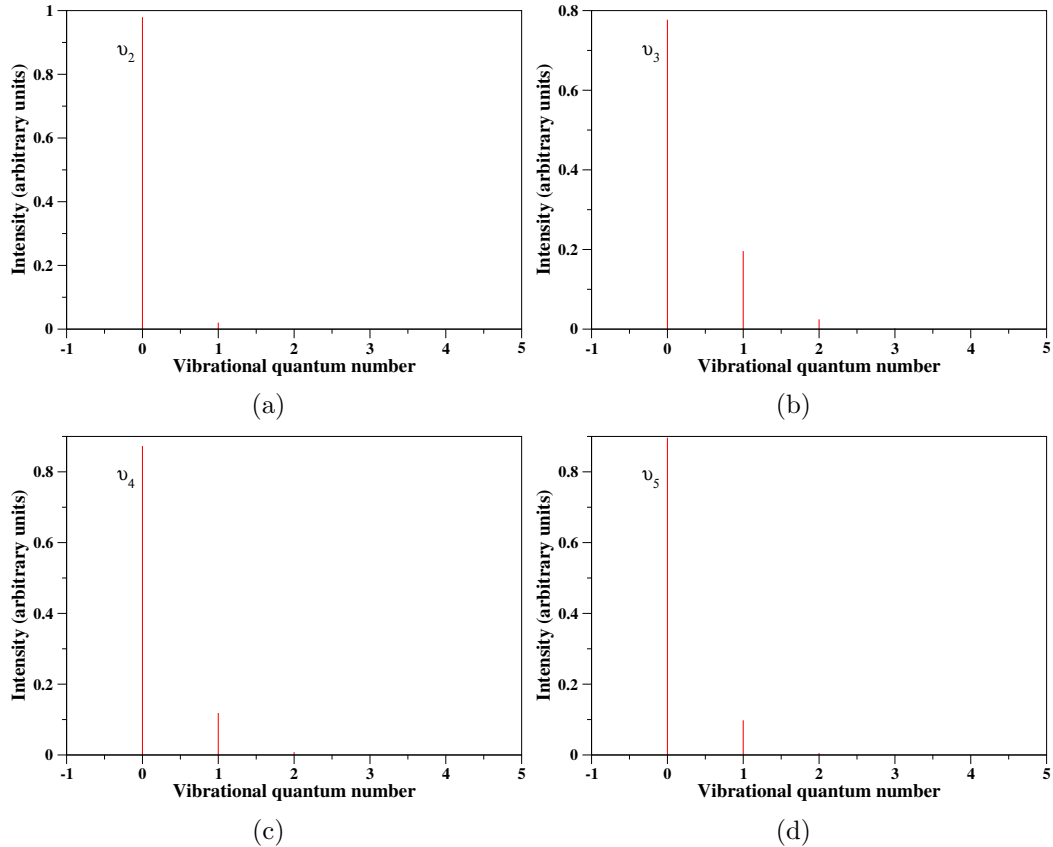


Figure S6. Poisson intensity distribution for tuning modes of \tilde{D}^2B_1 electronic state of Al_6N along vibrational quantum number.

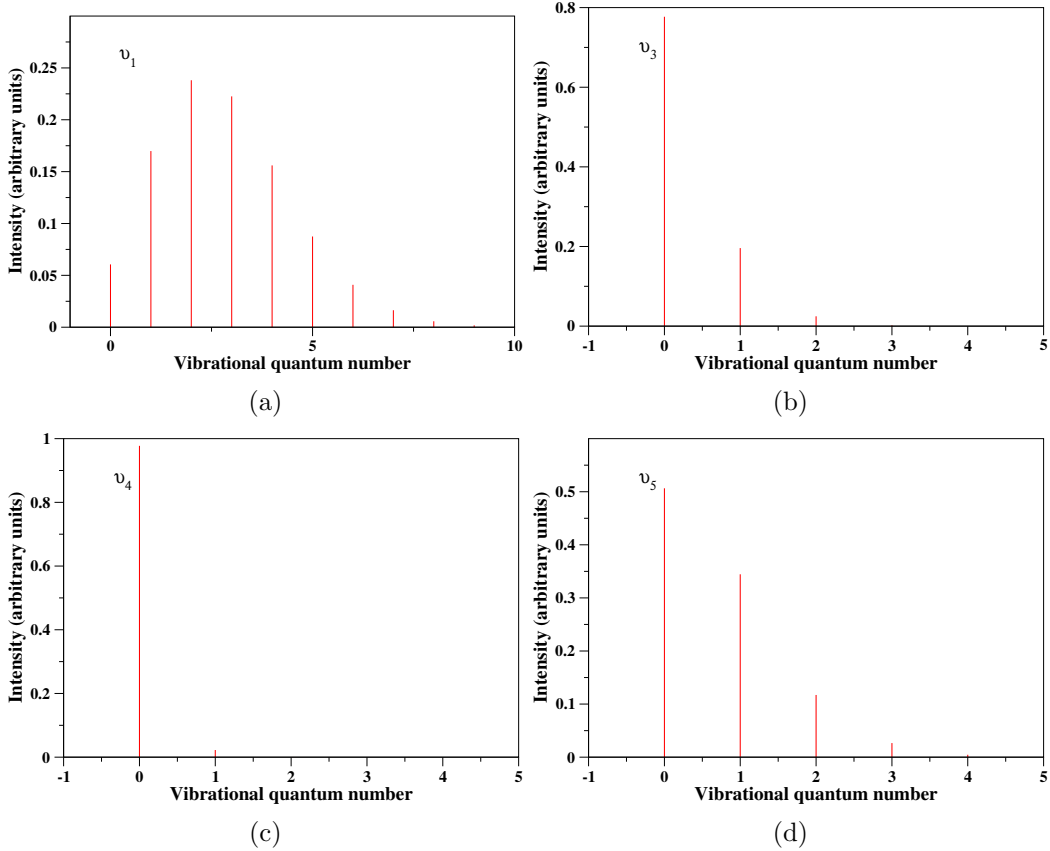


Figure S7. Poisson intensity distribution for tuning modes of $\tilde{E}^2 A_1$ electronic state of Al_6N along vibrational quantum number.

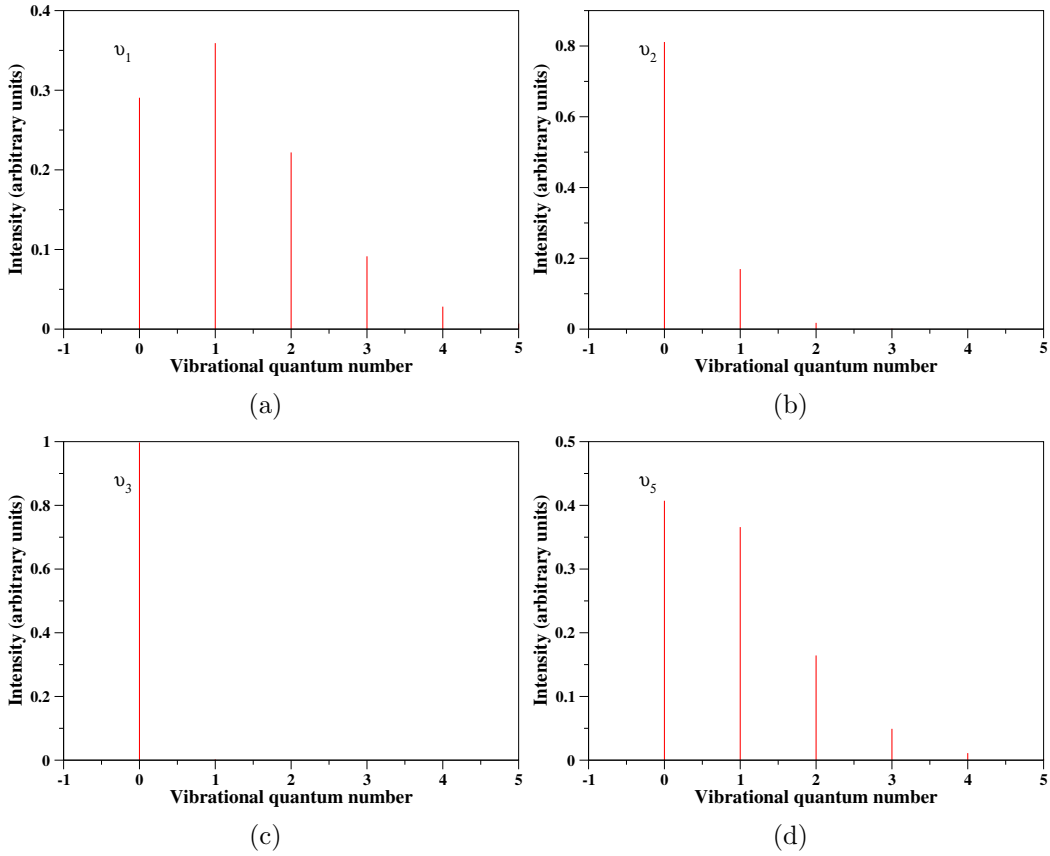


Figure S8. Poisson intensity distribution for tuning modes of \tilde{F}^2B_2 electronic state of Al_6N along vibrational quantum number.

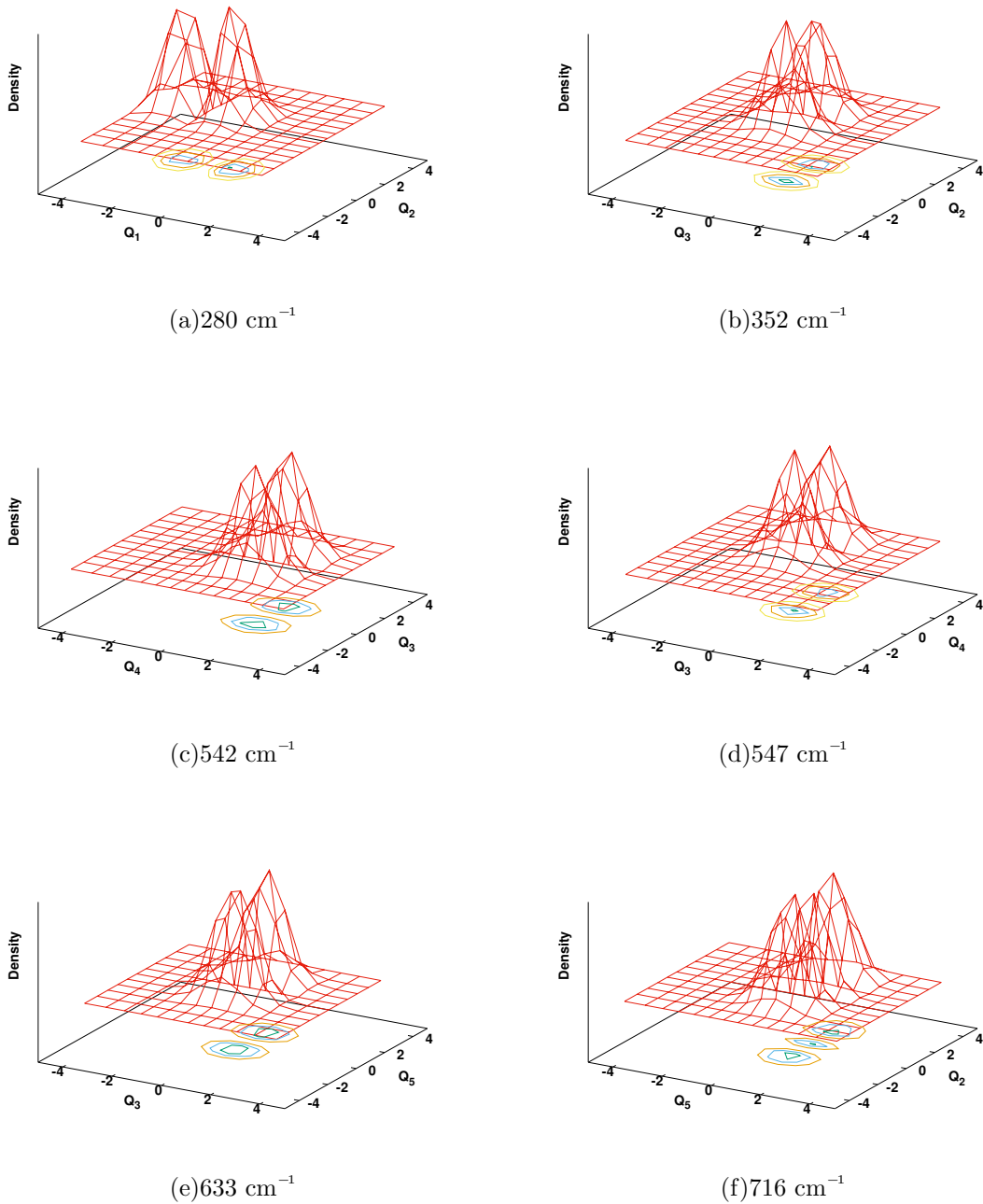


Figure S9. WP density plot for assignment of fundamental and first overtone of corresponding tuning modes for ground electronic state \tilde{A} .

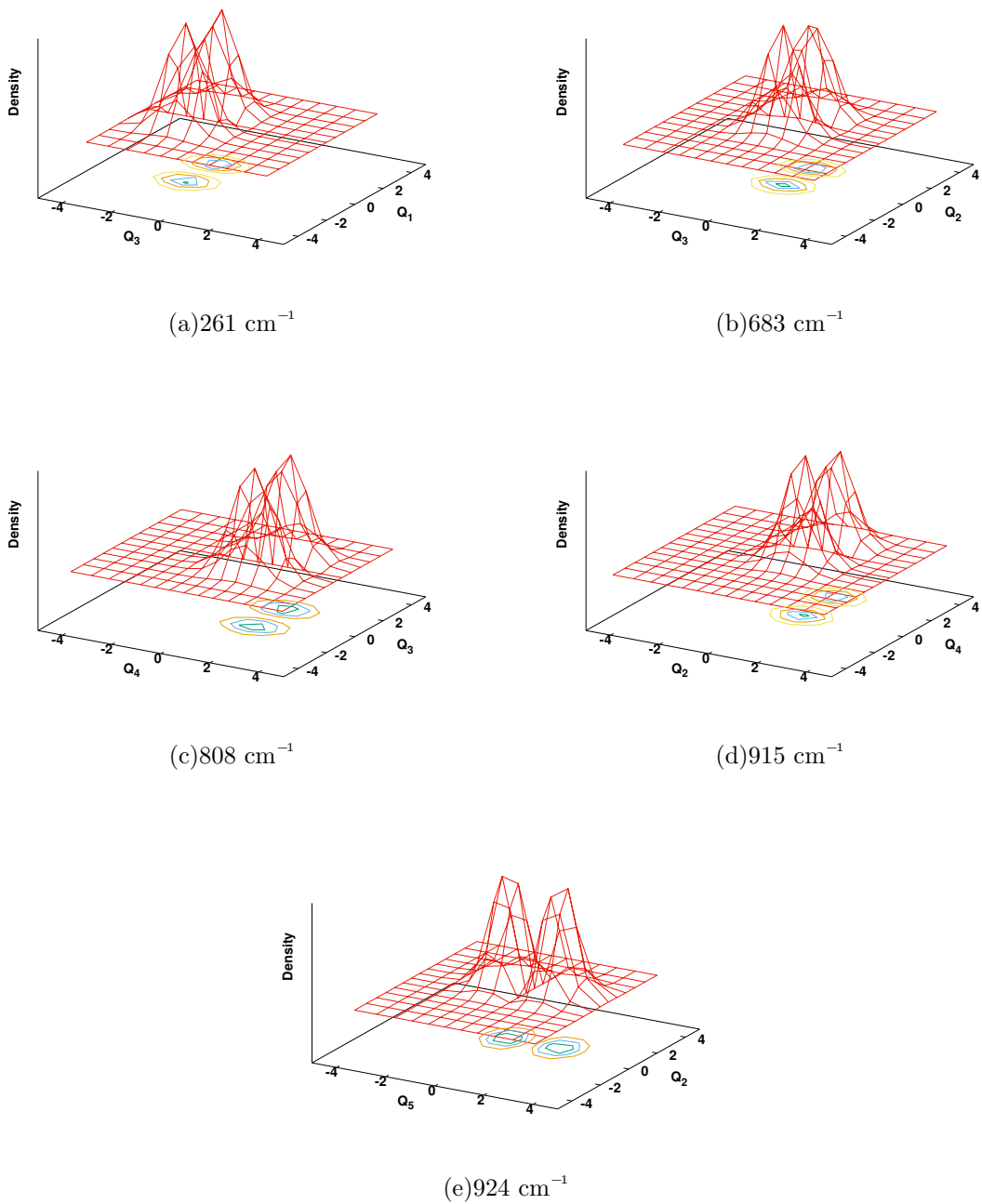


Figure S10. WP density plot for assignment of fundamental bands of corresponding tuning modes for \tilde{B} state.

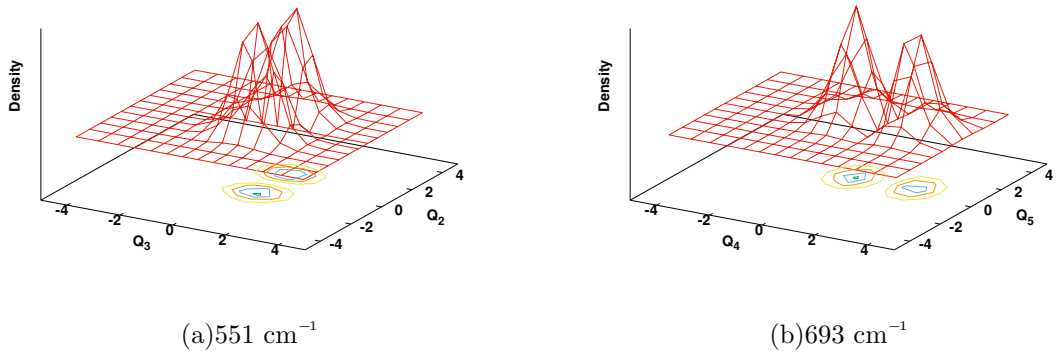


Figure S11. WP density plot for assignment of fundamental bands of corresponding tuning modes for \tilde{C} state.

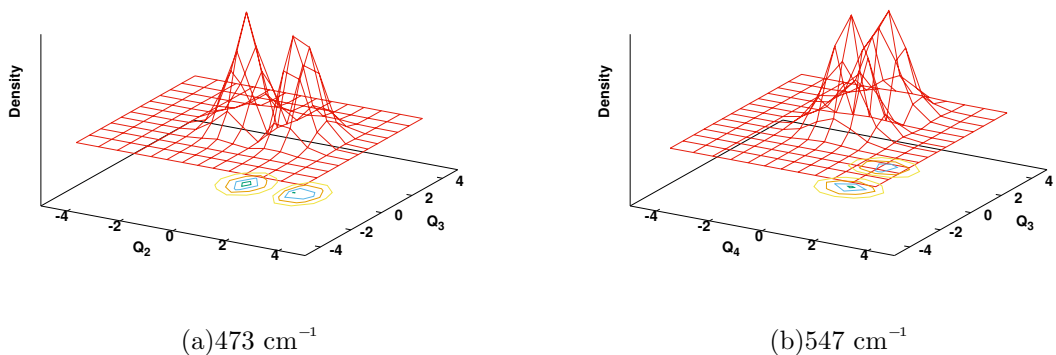


Figure S12. WP density plot for assignment of fundamental bands of corresponding tuning modes for \tilde{D} state.

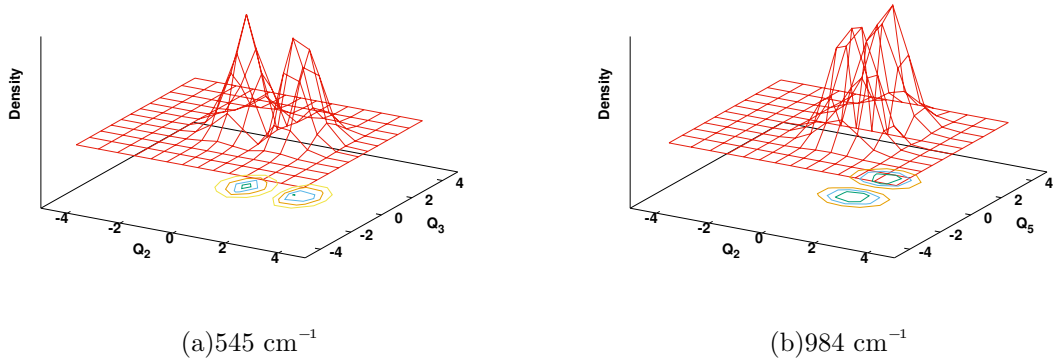


Figure S13. WP density plot for assignment of fundamental bands of corresponding tuning modes for \tilde{E} state.

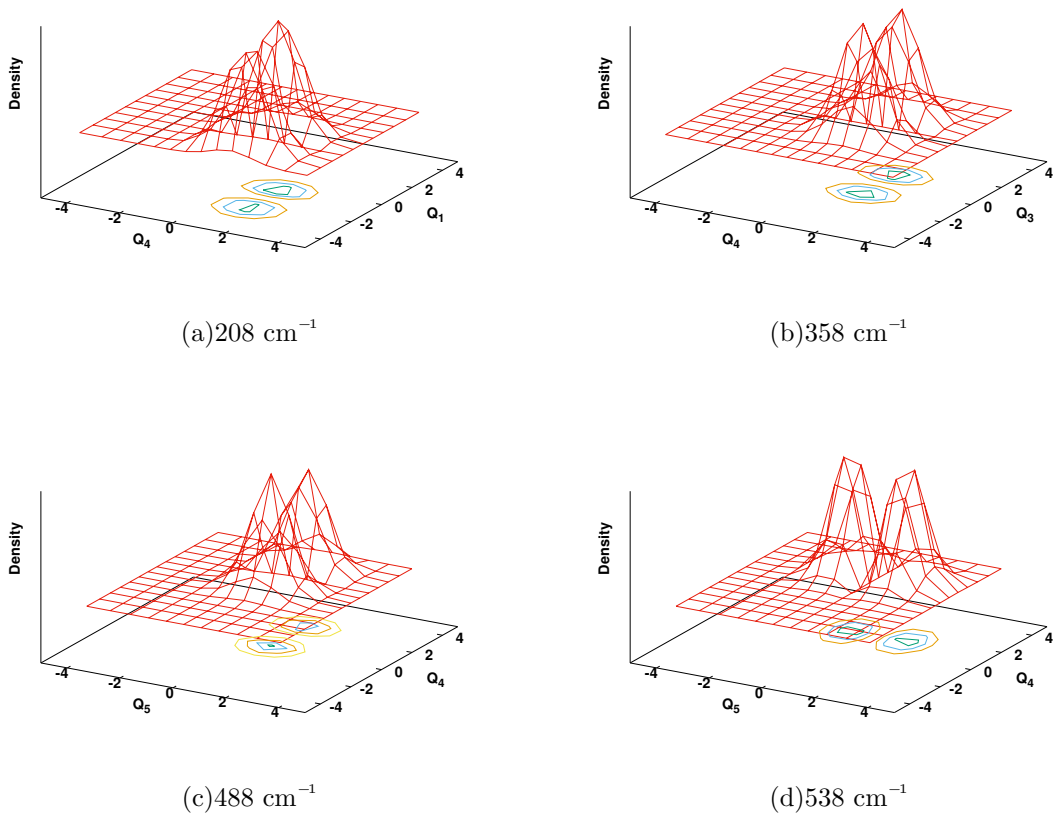


Figure S14. WP density plot for assignment of fundamental bands of corresponding tuning modes for \tilde{F} state.

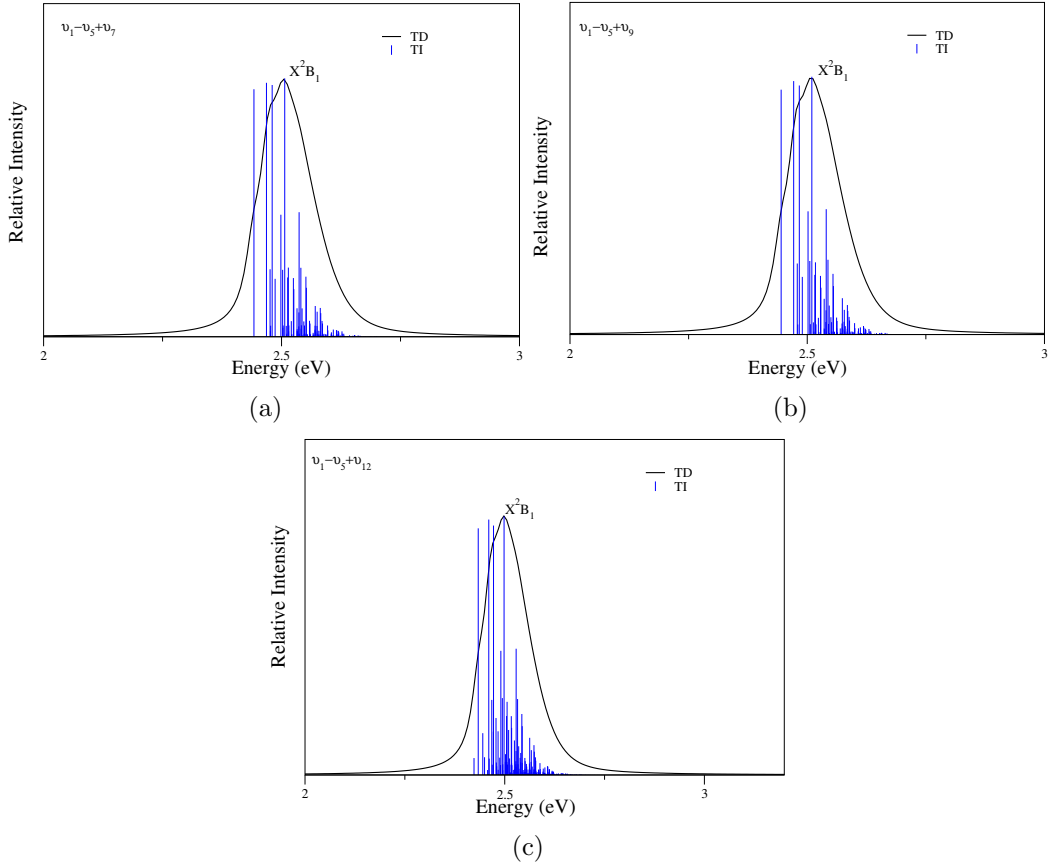


Figure S15. Comparison of TD and TI spectra for \tilde{X}^2B_1 electronic state including v_6 , v_7 , v_9 and v_{12} vibrational modes along with totally symmetric vibrational modes for Al₆N.

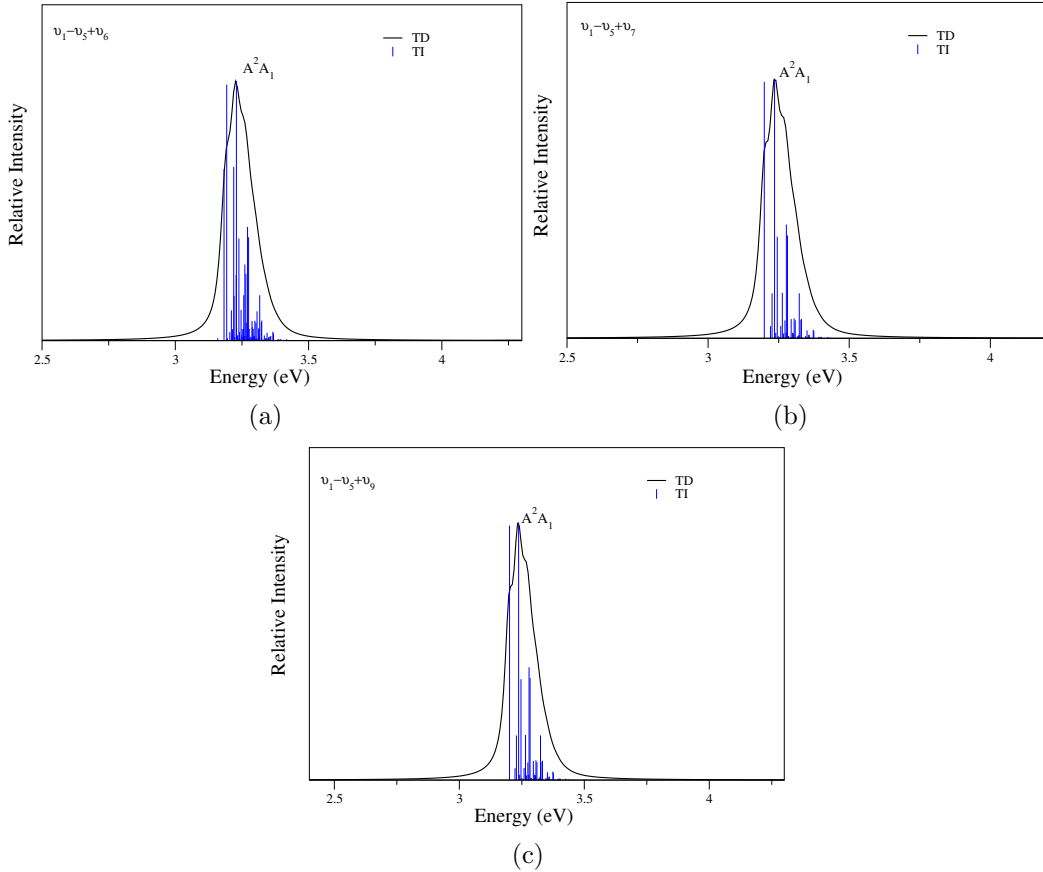


Figure S16. Comparison of TD and TI spectra for \tilde{A}^2A_1 electronic state including ν_6 , ν_7 and ν_9 vibrational mode along with totally symmetric vibrational modes for Al₆N.

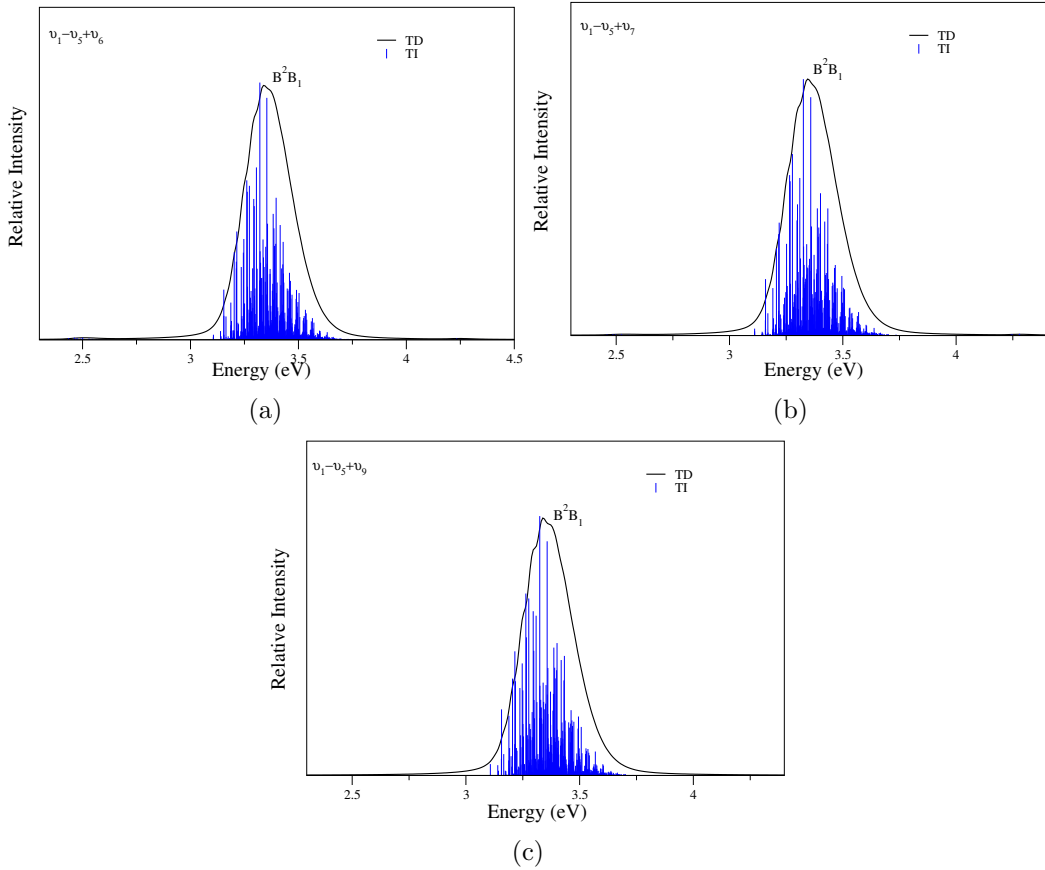


Figure S17. Comparison of TD and TI spectra for \tilde{B}^2B_2 electronic state including ν_6 , ν_7 and ν_9 vibrational mode along with totally symmetric vibrational modes for Al_6N .

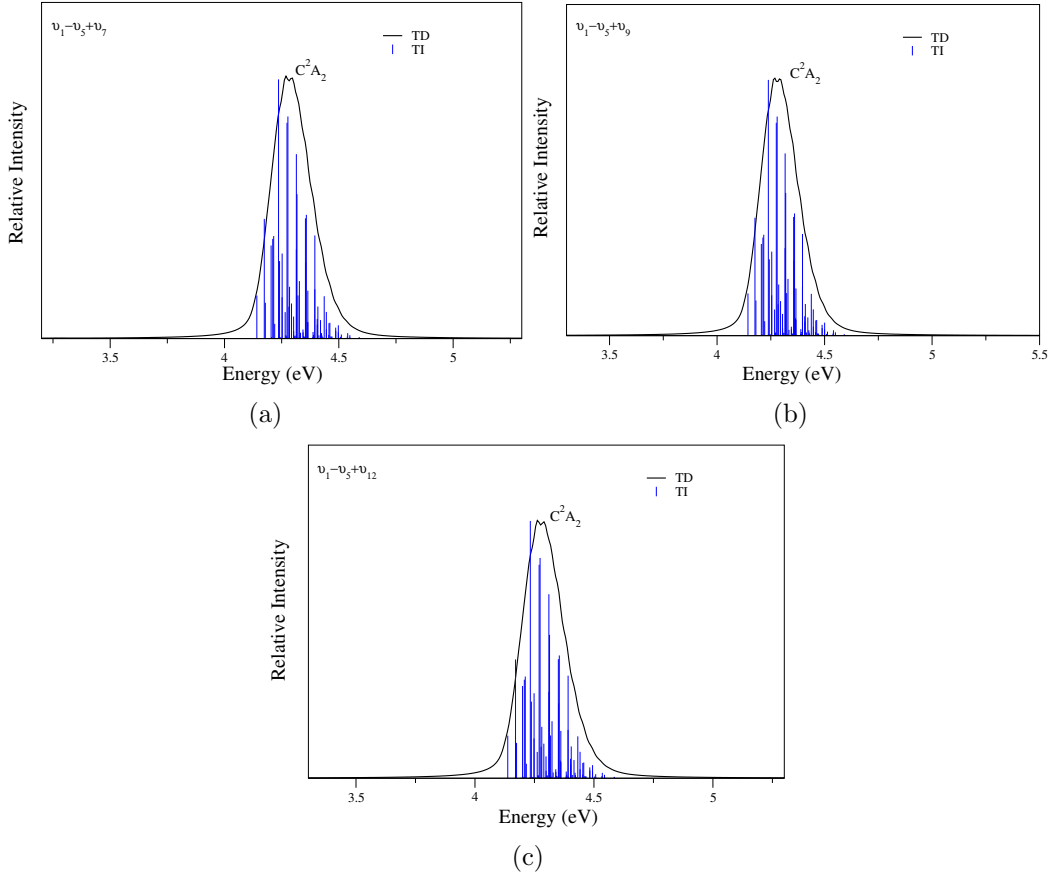


Figure S18. Comparison of TD and TI spectra for \tilde{C}^2A_2 electronic state including ν_6 , ν_7 , ν_9 and ν_{12} vibrational mode along with totally symmetric vibrational modes for Al₆N.

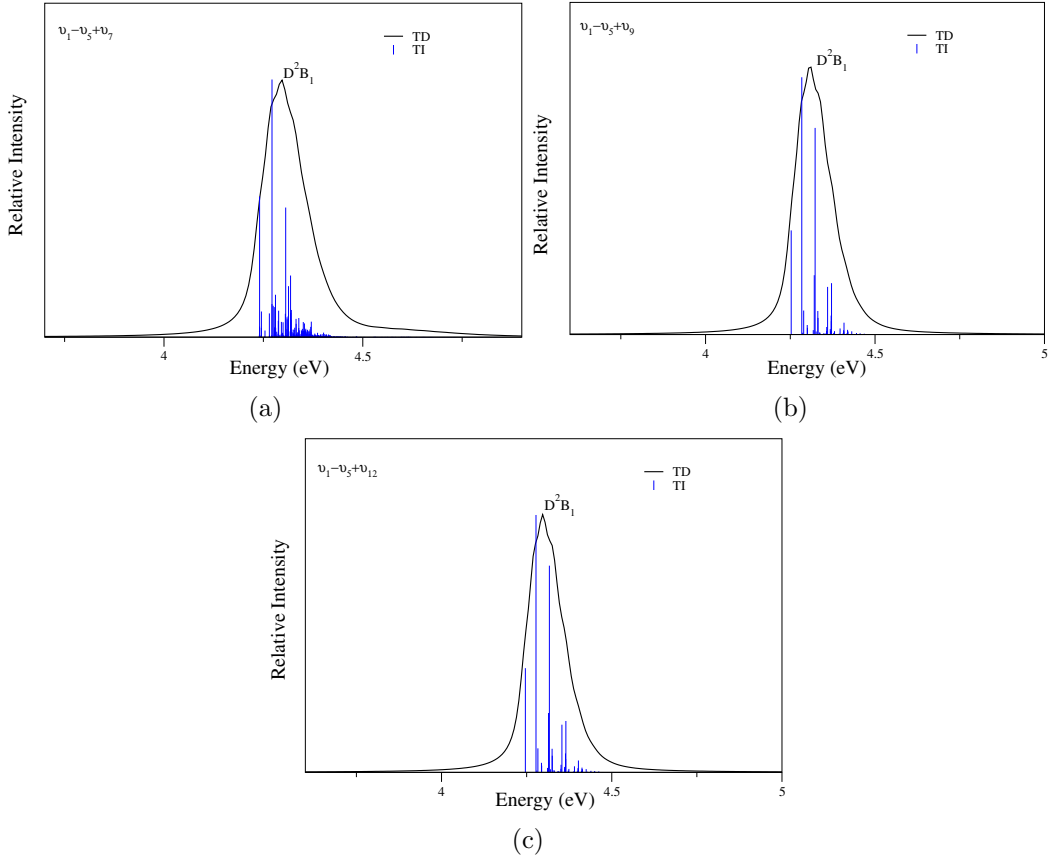


Figure S19. Comparison of TD and TI spectra for \tilde{D}^2B_1 electronic state including v_9 and v_{12} vibrational mode along with totally symmetric vibrational modes for Al_6N .

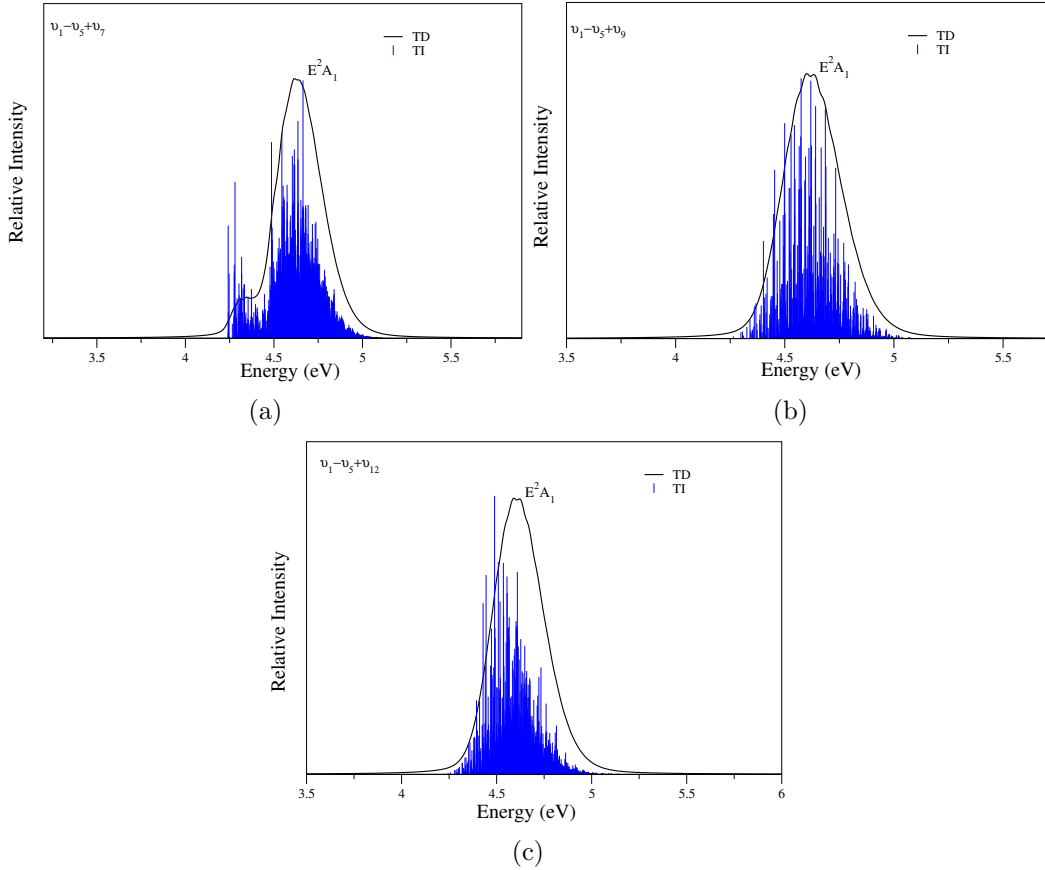


Figure S20. Comparison of TD and TI spectra for $\tilde{E}^2 A_1$ electronic state including ν_9 and ν_{12} vibrational mode along with totally symmetric vibrational modes for Al_6N .

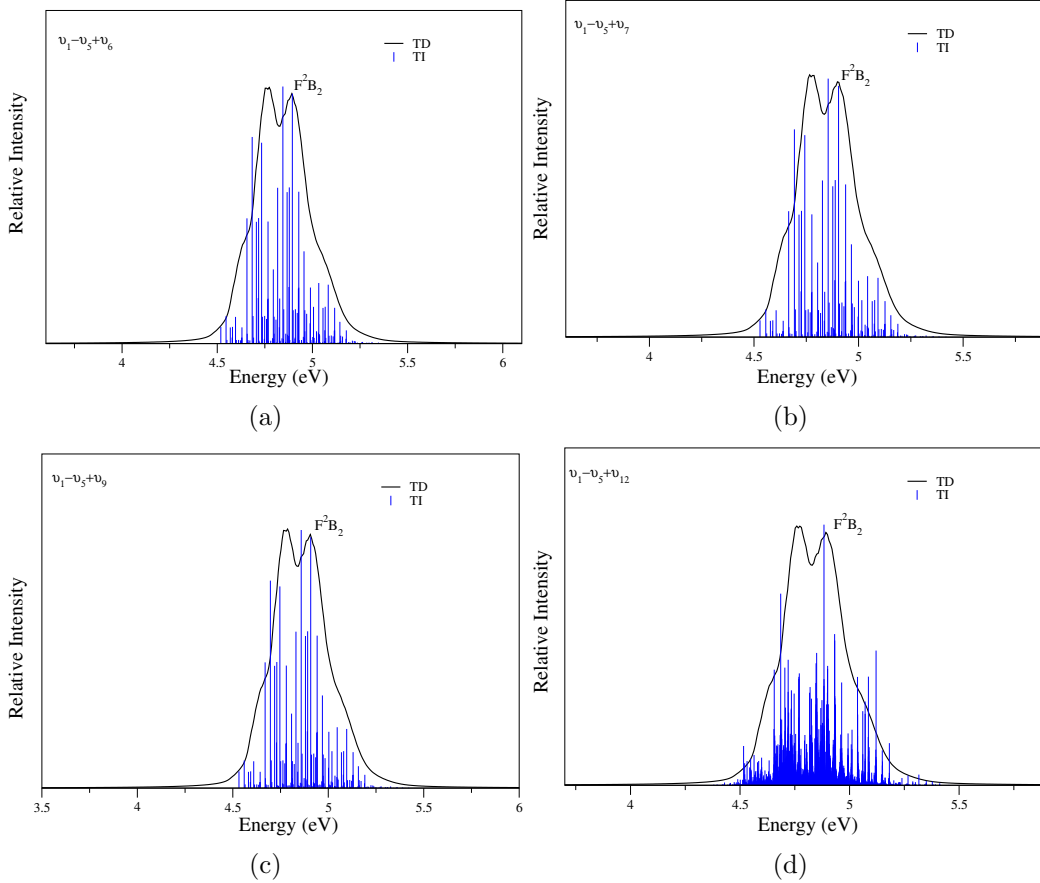


Figure S21. Comparison of TD and TI spectra for \tilde{F}^2B_2 electronic state including ν_6 , ν_7 , ν_9 and ν_{12} vibrational mode along with totally symmetric vibrational modes for Al₆N.